Proceedings of ASME FEDSM'03
4th ASME_JSME Joint Fluids Engineering Conference
Honolulu, Hawaii, USA, July 6-10, 2003

FEDSM2003-45166

LATTICE BOLTZMANN SIMULATION OF DROPS IN A SHEAR FLOW

Naoki Takada
National Institute of Advanced Industrial Science and Technology (AIST), Onogawa, Tsukuba 305-8569, Japan
naoki-takada@aist.go.jp

Akio Tomiyama , Shigeo Hosokawa
Graduate School of Science and Technology,
Kobe University, Rokkodai, Nada, Kobe 657-8501,Japan
tomiyama@mech.kobe-u.ac.jp

ABSTRACT

In this paper, we present simulation results of two- and three-dimensional motions of drops in a shear flow based on the lattice Boltzmann method (LBM), where a macroscopic fluid flow results from averaging collisions and propagations of mesoscopic particles. The binary fluid model in LBM used here can reproduce two-phase interface in a self-organizing way by repulsive interaction between particles consistent with the van der Waals-Cahn-Hilliard free energy theory. A finite difference scheme is applied to the lattice-Boltzmann equations governing time evolution of velocity distributions of particle number density. When a drop is suspended in an immiscible second liquid with the same mass and viscosity between moving parallel plates, the numerical results of deformation of drop agree with theoretical solutions and previous numerical results obtained by the volume-of-fluid (VOF) method. Breakup motions of drops in LBM are also reasonable in comparison with the critical Reynolds and capillary numbers predicted by the VOF method. In the simulations of two-drop interaction, it is shown that the breakup motion depends on not only number density of drops but also initial positioning of their volumetric center away from a halfway cross section between the plates.

INTRODUCTION

In recent years, the lattice Boltzmann method, LBM [1][2], has been developed as an alternative approach for simulating incompressible fluid flows and modeling physics of fluids, on statistical-thermodynamic assumptions that a fluid involves mesoscopic particles repeating collisions and propagations, and that the distributions of particles converge to a state of local equilibrium. The main advantages of the LBM, originated from the lattice gas cellular automaton method[3], are relatively easy implementation of boundary condition for solid surface with geometrical complexity, high efficiency on parallel computing, and self-organizing reproduction of interface. These are provided by the kinetic equations of particles that possesses linear convection (or streaming) operator in velocity space, local collision operator and repulsive interaction between particles. The LBM describes macroscopic variables by averaging the motion of particles from which the Navier-Stokes (NS) equations can be recovered through the chapman-Enskog expansion technique. Unlike conventional numerical methods based on the discretizations of the incompressible NS equations, the pressure in the LBM is calculated by using only the equation of sate, without solving the Poisson equation which requires time-consuming treatment.

The gas-liquid model [4] has been proposed to simulate isothermal phase changes consistent with the thermodynamic theory of van der Waals-Cahn-Hillard free energy. After that, the free-energy approach was also applied to the binary fluid model [5][6], called BF model hereafter. In an enhanced gas-liquid model [7], the Galilean invariance is improved remarkably. A novel thermal model [8][9] can simulate non-ideal two-phase fluid flows with phase change and heat transfer. The concept of the free-energy approach in the above-mentioned models is the same as that in the second gradient method (SGM) for the direct numerical simulation of liquid-vapor flows using the NS equations [10]. In both of the LBM and the SGM, an interface corresponds to a volumetric transient zone across which physical properties of fluid (i.e. density and viscosity) vary continuously, and the surface tension is reproduced from the energy contribution due to density gradient without the continuous surface force model.

So far, to examine applicability of the LBM in numerical analysis of two-phase fluid motions under gravity, we have considered the buoyancy effect on characterized with the non-dimensional numbers, and developed the three-dimensional BF model [11][12]. The results of two-dimensional bubble motions by the LBM agreed with those by the volume-of-fluid (VOF) method [13], and the surface tension in the 3D model obeyed the Laplace's law. It has been also verified that the BF model reproduces two-bubble coalescence and the effect of wall boundary on lateral motion of bubble in a vertical tube [14].

In this paper, we present numerical results of 2D and 3D motions of drops in a shear flow between moving parallel plates by using the lattice-Boltzmann BF model, with the immiscible two-phase scheme and the independent parameters for surface tension and interfacial thickness [15]. The purpose is to investigate deformation and rupture of two-phase interface under simple shear stress for generating fine drops. It is

important to understand deformation and breakup mechanisms of drops fundamentally in designing industrial- and environmental-use fluid devices. In the next section, the basis of the lattice-Boltzmann binary fluid model is described. After explaining a three-dimensional velocity distribution model and the improvement schemes for the BF model, the numerical results of drop deformation and breakup are shown in comparison with those by the VOF method [16] and theoretical solutions [17]. In addition to the above verification, the results of three-dimensional two-drop interaction are also presented. All of the simulations have been conducted under the conditions that both of mass density and viscosity ratios are 1.0 in isothermal two-phase fluids.

NOMENCLATURE

c	minimum speed of particles
Ca	capillary number
d_D	diameter of drop
$\mathbf{e}$	velocity vector of fluid particles
f	velocity distribution function of total number density of particles
g	velocity distribution function of number density difference of particles between two components
n	total number density of two-component particles
P	pressure
$\mathbf{r}$	position vector
Re	Reynolds number
T	temperature of fluid
$\mathbf{u}$	flow velocity

Greek Letters

Δn	particle number density difference between components
Δt	time increment
$\Delta\mu$	chemical potential difference
Γ	mobility parameter
κ	capillary coefficient
σ	surface tension
ν	kinetic viscosity of fluid
τ_1	relaxation time of collision operator for f
τ_2	relaxation time of collision operator for g

Subscript

a	label to distinguish fluid particles by their velocity
i	direction along lattice link line
l	index of particle speed in three dimensions
α,β	index of Cartesian coordinate

Superscript

eq	state of equilibrium

LATTICE-BOLTZMANN BINARY FLUID MODEL

To model interfacial dynamics of two-phase fluids, the binary fluid (BF) model [5] associates a repulsive interaction between two kinds of fluid particle components A and B with the free energy theory. In the BF model, two independent macroscopic variables are introduced to compute pressure and phase distribution, total number density $n = n_A + n_B$, and its difference $\Delta n = n_A - n_B$, which are related with two sets of the velocity distribution function of particle number density, f_a and g_a, respectively. The subscript a denotes the label to distinguish the particles by their velocity vectors $\mathbf{e}_a$. The variables, n, Δn, and flow velocity $\mathbf{u}$ are defined with the functions as follows,

$$n = \sum_a f_a = \sum_a f_a^{eq}, \tag{1}$$

$$\Delta n = \sum_a g_a = \sum_a g_a^{eq}, \tag{2}$$

$$n\mathbf{u} = \sum_a f_a \mathbf{e}_a = \sum_a f_a^{eq} \mathbf{e}_a, \tag{3}$$

$$\Delta n\,\mathbf{u} = \sum_a g_a^{eq} \mathbf{e}_a, \tag{4}$$

where the superscript eq denotes an equilibrium distribution. The total density n is proportional to pressure and approximately constant in whole flow field, while the density difference Δn takes either positive or negative values in each phase and then represent phase distributions.

The time evolution of discrete velocity distributions of particle number density is governed by the lattice Boltzmann equations (LBE). The differential forms of LBE in the BF model are written as follows,

$$\frac{\partial f_a(t,\mathbf{r})}{\partial t} + \mathbf{e}_a \cdot \nabla f_a(t,\mathbf{r}) = -\frac{1}{\tau_1}\left[f_a(t,\mathbf{r}) - f_a^{eq}(t,\mathbf{r})\right] \tag{5}$$

$$\frac{\partial g_a(t,\mathbf{r})}{\partial t} + \mathbf{e}_a \cdot \nabla g_a(t,\mathbf{r}) = -\frac{1}{\tau_2}\left[g_a(t,\mathbf{r}) - g_a^{eq}(t,\mathbf{r})\right] \tag{6}$$

where $\mathbf{r}$ is the position vector, τ_1 and τ_2 are the relaxation times. After collision at a site $\mathbf{r}$, the particles with $\mathbf{e}_a$ move to its neighbors $\mathbf{r}+\mathbf{e}_a$ during unit time period. The terms on the right hand sides of Eqs.(5) and (6), so-called lattice BGK collision operators [2], indicate the relaxation process toward states of local equilibrium f_a^{eq} and g_a^{eq}. The macroscopic variables, n, Δn, and $n\mathbf{u}$, are conserved at each site in every collision step.

The thermodynamic behavior of binary fluid system in the BF model is governed by a simple free energy Ψ including the energy contribution from density gradient [6],

$$\Psi = \int d\mathbf{r}\left\{\psi(T,n,\Delta n) + \frac{\kappa}{2}|\nabla \Delta n|^2\right\}, \tag{7}$$

$$\psi = \frac{T_C}{2}\left(n - \frac{\Delta n^2}{n}\right) - nT + \frac{T}{2}\left[(n+\Delta n)\ln\left(\frac{n+\Delta n}{2}\right) + (n-\Delta n)\ln\left(\frac{n-\Delta n}{2}\right)\right], \tag{8}$$

where κ is the capillary coefficient to control surface tension and interfacial thickness, and T_C is critical temperature. When $T<T_C$, an isothermal fluid system in the BF model goes through two-phase separation and coexistence, where each phase corresponds to component-A-rich or B-rich region.

The function Ψ Eq.(7) is related with the pressure tensor $P_{\alpha\beta}$ and the chemical potential difference $\Delta\mu$,

$$P_{\alpha\beta} = P\delta_{\alpha\beta} + \kappa \frac{\partial \Delta n}{\partial x_\alpha}\frac{\partial \Delta n}{\partial x_\beta}, \tag{9}$$

$$P = \Delta n \frac{\delta\psi}{\delta \Delta n} - \Psi = nT - \kappa\left(\Delta n \nabla^2 \Delta n + \frac{|\nabla \Delta n|^2}{2}\right), \tag{10}$$

$$\Delta\mu = \frac{\delta\Psi}{\delta\Delta n} = -T_C\frac{\Delta n}{n} + \frac{T}{2}\ln\left(\frac{1+\Delta n/n}{1-\Delta n/n}\right) - \kappa\nabla^2(\Delta n), \tag{11}$$

where the Greek subscripts are Cartesian coordinate indices and $\delta_{\alpha\beta}$ is the symbol of Kronecker's delta. These thermodynamic quantities are embedded into the equilibrium velocity distributions f_a^{eq} and g_a^{eq} through the following relations,

$$P_{\alpha\beta} = \sum_a f_a^{eq}\left(e_{a\alpha} - u_\alpha\right)\left(e_{a\beta} - u_\beta\right), \tag{12}$$

$$\Gamma\Delta\mu\delta_{\alpha\beta} = \sum_a g_a^{eq}\left(e_{a\alpha} - u_\alpha\right)\left(e_{a\beta} - u_\beta\right), \tag{13}$$

where Γ is parameter of mobility.

The macroscopic dynamics of binary fluids can be derived from the LBE (5) and (6) through the Chapman-Enskog's multi-scale expansion technique [2]. The former is related with the continuum equation and the equation of motion of two-phase fluid with unit mass density, while the latter leads to the convection-diffusion equation for the function Δn.

3D EQUILIBRIUM DISTRIBUTION OF PARTICLES

In this study, three-dimensional particle velocity distribution adopts an isotropic velocity set including rest component, as shown in Fig.1 [10]. Subscript a of the distribution functions is replaced with l and i. The former l =1,2 is identification index of two speeds $c(l+1)^{1/l}$, while i is index of the velocity directions: i=1 to 6 for l=1, i=1 to 8 for l=2. Generally, c =1 is used because of normalization of speed.

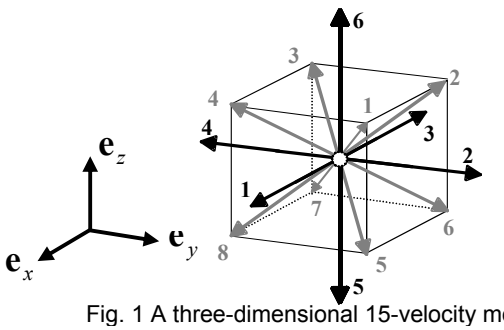

Fig. 1 A three-dimensional 15-velocity model.

The equilibrium distributions $f_{l,i}^{eq}$ and $g_{l,i}^{eq}$ are represented on the limit of low Mach number by the following forms,

$$f_{li}^{eq} = n\left[A_l + \frac{B_l}{c^2}\mathbf{e}_{li}\cdot\mathbf{u} + \frac{C_l}{c^4}\left(\mathbf{e}_{li}\cdot\mathbf{u}\right)^2 + \frac{D_l}{c^2}\mathbf{u}\cdot\mathbf{u}\right] + G_{\alpha\beta}^{(l)}e_{li\alpha}e_{li\beta}, \tag{14}$$

$$f_0^{eq} = n\left[A_0 + \frac{D_0}{c^2}\left(\mathbf{u}\cdot\mathbf{u}\right)\right], \tag{15}$$

$$g_{li}^{eq} = \frac{B_l\Gamma\Delta\mu}{c^2} + \Delta n\left[\frac{B_l}{c^2}\left(\mathbf{e}_{li}\cdot\mathbf{u}\right) + \frac{C_l}{c^4}\left(\mathbf{e}_{li}\cdot\mathbf{u}\right)^2 + \frac{D_l}{c^2}\left(\mathbf{u}\cdot\mathbf{u}\right)\right], \tag{16}$$

$$g_0^{eq} = \Delta n - \frac{6B_1 + 8B_2}{c^2}\Gamma\Delta\mu + \frac{D_0}{c^2}\Delta n\left(\mathbf{u}\cdot\mathbf{u}\right), \tag{17}$$

where Eqs.(15) and (17) correspond to the distribution functions for rest particles. The dimensionless parameters A_l, B_l, C_l, and D_l, and the tensor $G_{\alpha\beta}^{(l)}$ are determined under the constraints to derive the Navier-Stokes equations with the pressure tensor Eq.(12) from the LBE, Eq.(5) [11]. A_l (l=1,2), A_0 and $G_{\alpha\beta}^{(l)}$ (l=1,2) take the following forms respectively,

$$A_l = \frac{s_l}{8(s_1+s_2)c^2}\left[T - \kappa\frac{\Delta n}{n}\nabla^2\Delta n\right], \tag{18}$$

$$A_0 = 1 - 6A_1 - 8A_2, \tag{19}$$

$$G_{\alpha\beta}^{(l)} = \frac{\kappa}{c^4}\left[E_l\frac{\partial\Delta n}{\partial r_\alpha}\frac{\partial\Delta n}{\partial r_\beta} + F_l\left|\nabla\Delta n\right|^2\delta_{\alpha\beta}\right]. \tag{20}$$

In Eq.(18), s_l denotes the number density ratio of particles with speed $2c$ and $\sqrt{3}\,c$, in a rest equilibrium state at temperature,

$$T = 8(s_1 + s_2)c^2. \tag{21}$$

The following set of parameters are used in this study: B_1 = 1/24, B_2 = 1/12, C_1 = 1/32, C_2 = 1/16, D_0 = -7/24, D_1 = -1/48, D_2 = -1/24, E_1 = 1/32, F_1 = -1/32, E_2 = 1/16, and F_2 = 0.

IMPROVEMENT OF BINARY FLUID MODEL

This section describes the schemes in the BF model to simulate the motions of immiscible two-phase fluids under more flexible control of surface tension and interfacial thickness [13][14]. First, the convection term in the LBE for the function g_a, Eq.(6), is replaced with new version of the local equilibrium one g_a^{eq} to reduce the diffusivity of Δn due to phase change inherent in the original BF model[5], as follows,

$$\frac{\partial g_a(t,\mathbf{r})}{\partial t} + \mathbf{e}_a\cdot\nabla g_a^{eq}(t,\mathbf{r}) = -\frac{g_a(t,\mathbf{r}) - g_a^{eq}(t,\mathbf{r})}{\tau_2}. \tag{22}$$

where τ_2 takes values equal to time increment Δt.

Second, two independent parameters κ_1 and κ_2 are introduced into the pressure tensor and the chemical potential difference, Eqs.(9) and (11) respectively, instead of a common capillary coefficient κ. Surface tension σ is obtained from the following mechanical definition on a flat interface perpendicular to x axis in Cartesian coordinate,

$$\sigma \equiv \int_{-\infty}^{+\infty}\left(P_N - P_L\right)dx = \kappa_1\int_{-\infty}^{+\infty}\left(\frac{\partial\Delta n}{\partial x}\right)^2 dx, \tag{23}$$

where P_N=P_{xx} and P_L=P_{yy}=P_{zz}. An interfacial profile along x axis $\Delta n(x)$ is determined on the constraint that the chemical potential has to be constant all over flow region when the system reaches a state of thermodynamic equilibrium, that is,

$$-T_C\frac{\Delta n}{n} + \frac{T}{2}\ln\left(\frac{1+\Delta n/n}{1-\Delta n/n}\right) - \kappa_2\nabla^2(\Delta n) = constant, \tag{24}$$

$$T_C = \frac{nT}{2\Delta n_0}\ln\left(\frac{1+\Delta n_0/n}{1-\Delta n_0/n}\right), \tag{25}$$

where Δn_0 is positive value given in component-A-rich regions. Equation (24) means there is no net variation of number of particles in each phase. Figure 2 shows the theoretical predictions of the function Δn across a flat interface, which are obtained from solving Eq.(24) numerically. The interface, volumetric transient zone, becomes thinner and the gradient of Δn increases as κ_2 decreases. Substituting these results into Eq.(23), it is proved that the surface tension σ is inversely proportional to κ_2 and the thickness, as shown in Table.1.

In addition to the above schemes, the differential forms of the LBE (5) and (22) are discretized with the finite difference-based lattice Boltzmann method (FDLBM) [18]. The FDLBM can overcome numerical instability at high Reynolds number easily by time and physical space discretizations with arbitrary mesh configuration not to depend on particle velocity set so that the Courant number becomes smaller than 1 flexibly. In this study, we applied a third-order-accurate upwind difference scheme and the second-order-accurate Runge-Kutta's scheme with constant Δt to the convection term and the time marching

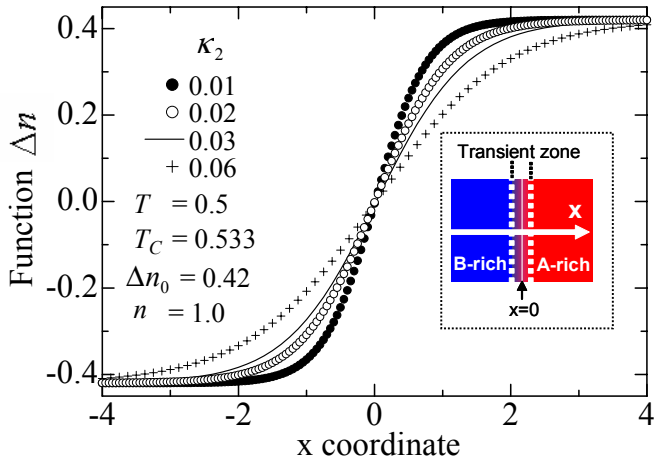

Fig. 2 Theoretical solution of thickness profile of a flat interface in the binary fluid model.

Table 1. Surface tension and density gradient for κ_2.

κ_2	σ/κ_1	Max. $\lvert\nabla\Delta n\rvert$
0.01	0.310	0.550
0.02	0.219	0.389
0.03	0.179	0.317
0.06	0.125	0.222

in the LBE. In the FDLBM, kinetic viscosity ν takes the following forms in the two-dimensional 7-velocity distribution [4] and the 3D 15-velocity distribution [10] respectively,

$$\nu = \frac{1}{4}\tau_1 c^2, \tag{26}$$

$$\nu = 8B_2\tau_1 c^2. \tag{27}$$

NUMERICAL RESULTS OF DROP MOTION

In this section, we present numerical results of motions of two- and three-dimensional drops in a simple Couette flow by the lattice-Boltzmann BF model. First of all, the results of drop deformation and breakup are shown in comparison with the previous numerical ones by the VOF method [16] and the solution of small deformation theory [17]. As shown in Fig.3, in the initial conditions, a circular- or spherical-shaped drop with diameter d_D =16 is suspended in a second immiscible liquid with the same density and viscosity on a halfway line between parallel plates moving with constant speed U_W in the opposite directions. In the Cartesian coordinate, the shear flow fields, which are discretized uniformly by square or cubic mesh with widths $\Delta x = \Delta y = \Delta z = 1$, possess plate separation H and spatial periodicities L_x and L_y. The extrapolation boundary condition [19] for f_a and g_a is applied to the plate boundaries.

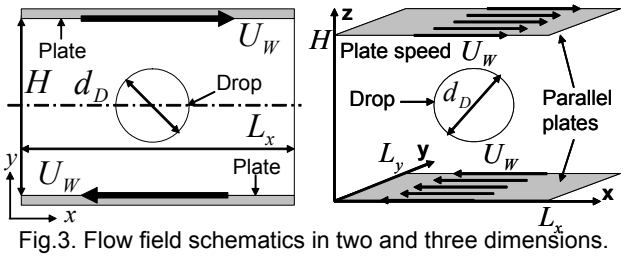

Fig.3. Flow field schematics in two and three dimensions.

The simulations were carried out under several conditions of non-dimensional numbers, Reynolds and capillary numbers Re and Ca, including two competing forces: viscous shear stress and the Laplace pressure $2\sigma/d_D$. They are defined by,

$$Re = \frac{\dot{\gamma}}{\nu}\left(\frac{d_D}{2}\right)^2, \quad Ca = \frac{\dot{\gamma}\nu d_D}{2\sigma}, \tag{28),(29)}$$

where $\dot{\gamma}$ is imposed shear rate, $2U_W/H$, and ν is kinetic viscosity given by Eqs.(26) and (27). Surface tension σ is determined with Eqs.(23) and (24) in advance. Before shear flow simulations, the surface tension of the improved BF model has been verified numerically through formation of a two-dimensional drop in stagnant liquid. Figure 3 shows pressure increment ΔP inside circular-shaped drop with radius $R = d_D/2$. $P_0 = nT$ is pressure outside drop, where values n=1 and T=0.5 are used in all of other simulations as well. The results by the lattice-Boltzmann BF model agree well with theoretical

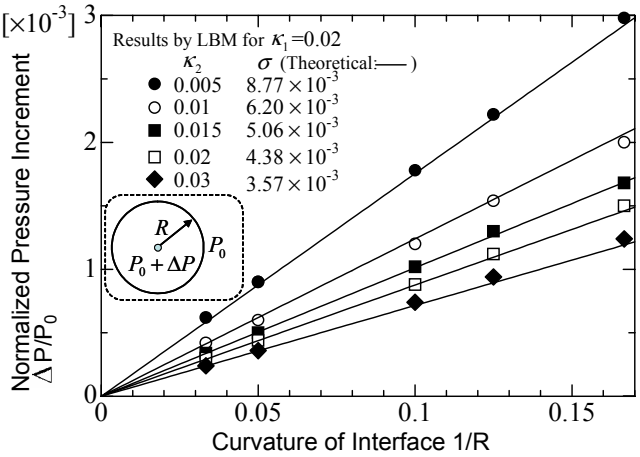

Fig.4. Pressure increments inside two-dimensional drop versus interfacial curvature.

predictions by the Laplace's law $\Delta P = 2\sigma/d_D$ in 2D and Eqs.(23) and (24). In the simulations mentioned hereafter, κ_2 is set to be 0.01 at the same values of n, Δn and T as the above.

In the first simulations of time-dependent shear flow, where matrix and drop liquids are stagnant initially, two parameters were used to measure the deformation attained by the drop in steady state at the low Reynolds numbers Re=0.333 in 2D and 0.0625 in 3D. The first one is the Taylor deformation parameter $D = (L-B)/(L+B)$, where L and B are the half-length and half-breadth of the drop, respectively (Fig.5). The second one is the orientation angle θ of the drop with the axis of shear strain.

The results of two parameters of drop deformation by the LBM are shown in Fig.6 and Fig.7, together with the previous

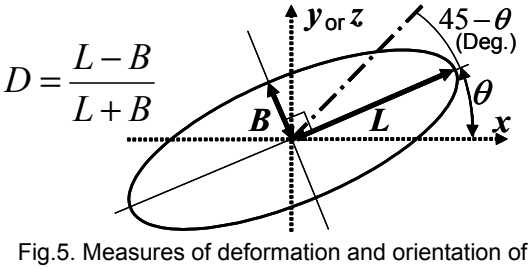

Fig.5. Measures of deformation and orientation of drop.

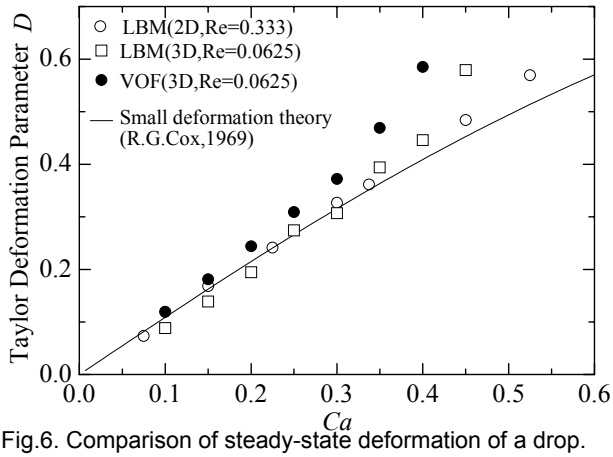

Fig.6. Comparison of steady-state deformation of a drop.

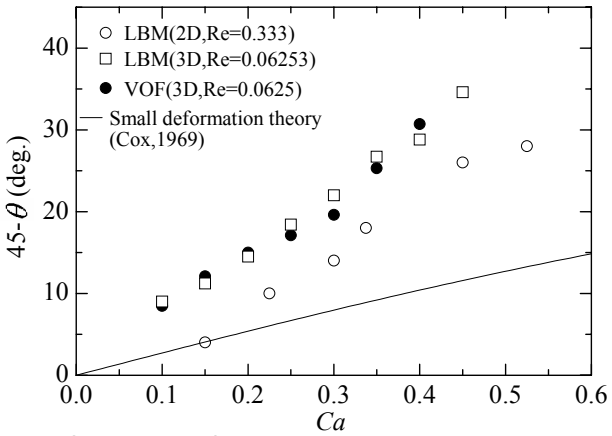

Fig.7. Comparison of the steady-state drop orientation angle θ.

ones [16][17]. The computational domain is rectangular box with H =128, L_x =64, and L_y =32 in Fig.4. The Taylor deformation parameters in the 3D LBM simulations agree with the theoretical solutions and numerical results obtained with the VOF method. On the other hand, in the higher capillary numbers, the deviation of the 2D results from the theoretical prediction is smaller than that of the 3D results. In terms of the orientation angle, there are good agreements between numerical results by the LBM and the VOF method in three dimensions.

The second simulation is breakup of drop with d_D =16, which were carried out in the computational domain with $H = L_x$=64 and L_y =32. Figure 8 depicts the diagram of drop breakup in the capillary-Reynolds plane. Compared with the results obtained with the VOF method, the LBM reproduces almost equal results to predict the critical capillary and Reynolds numbers in three dimensions. On the other hand, it is shown that the two-dimensional drop tends to break up at higher Reynolds number than the 3D drop at given capillary number. Figure 9 shows the interfacial profiles and the flow velocity fields on a x-z cross section at *y*=16 for *Ca*=0.3 and *Re*=0.01, 0.1, 0.5 and 0.6. As *Re* increases, the drop deformation becomes larger in the same way as the VOF method [16]. Although the values of the deformation parameter *D* became smaller than those in the previous simulations (Table.2), the LBM reproduced the increase of *D* with *Re* and the breakup of drop at *Re* =0.75, as shown in Fig.10.

The last numerical results, shown in Fig.11, are concerned with the two-drop interaction in the three-dimensional shear

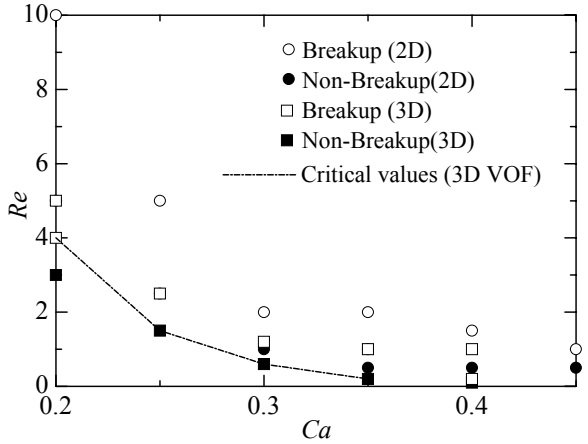

Fig.8. Diagram of two- and three- dimensional drop breakup at the capillary and Reynolds numbers.

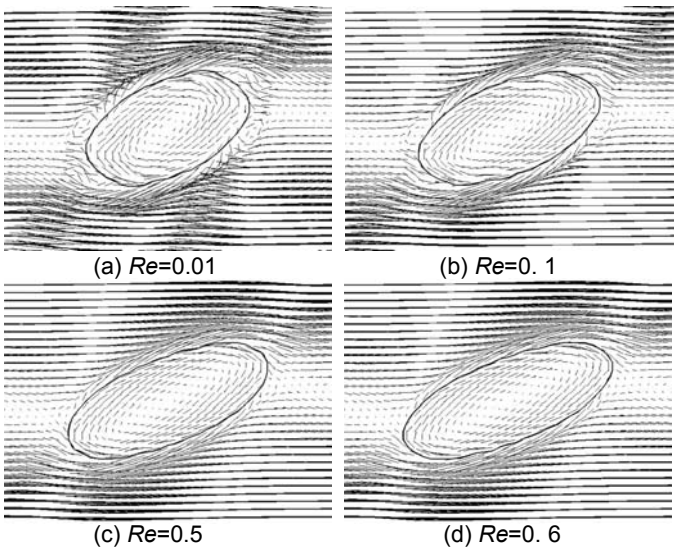

Fig.9. Steady-state solutions of interfacial profile and flow velocity on a cross section in x-z plane through the center of the drop at *Ca*=0.3.

Table 2. Taylor deformation parameter D in LBM simulation varied with *Re* at *Ca*=0.3, compared with results obtained with VOF method [16].

Re		0.0	0.1	0.5	0.6	0.75
D	LBM	0.279	0.347	0.429	0.459	break
	VOF	0.372	0.3869	0.45	0.4768	break

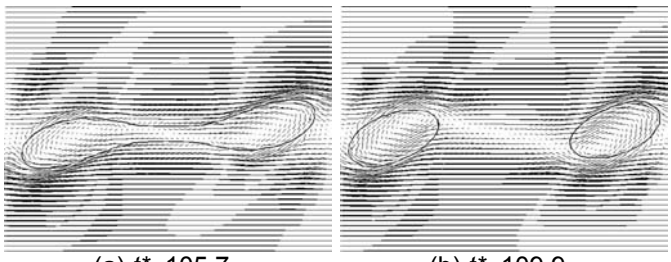

Fig.10. Snapshots of 3D drop breakup for *Ca*=0.3 and *Re*=0.75, at $t^* = t \times (2U_W / H)$. t is time in the flow field. Δt =0.25.

flow at *Ca* =0.3 and *Re* =1.0, using the same computational domain size and d_D as the above breakup simulations. In Case (a), when initially placed on a halfway x-y plane between plates, the drops do not break up to keep ellipsoidal-shaped. In contrast, they move in the opposite directions with each other to break up finally in Case (b), where their initial volumetric centers are placed away from the halfway plane by d_D. These results indicate that the critical *Ca* and *Re* for breakup of drops by shear stress depend on not only the spatial periodicity or number density of drops but also initial positioning of them to encourage the deformations as moving them with different speeds or directions.

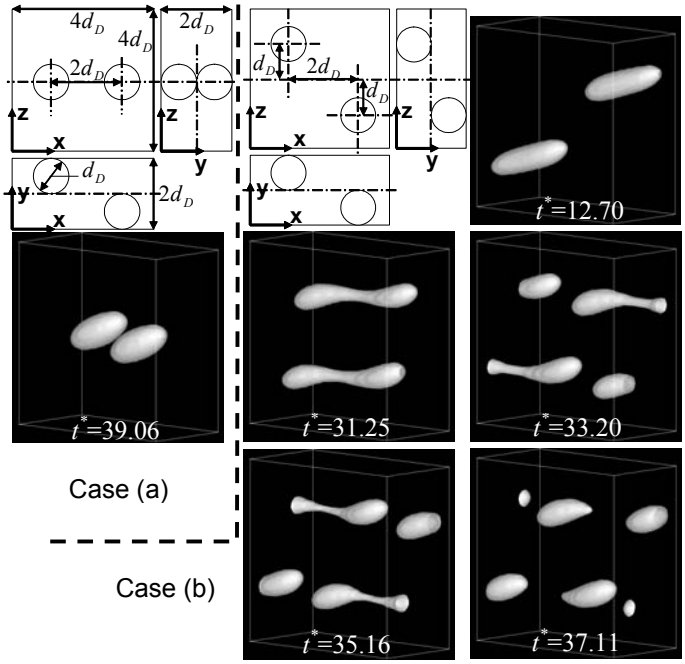

Fig.11. Initial conditions and snapshots of two-drop interaction for *Ca*=0.3 and *Re*=1 at dimensionless time $t^* = t \times (2U_W / H)$.

CONCLUSIONS

We carried out numerical simulations of motions of two- and three-dimensional drops in a shear flow based on the lattice-Boltzmann binary fluid model, which is consistent with the van der Waals-Cahn-Hilliard free energy theory. The model is improved for immiscible fluids with the finite difference scheme and the independent parameters to control surface tension and interfacial thickness. When a drop is suspended in a second liquid with the same mass and viscosity between moving parallel plates, the three-dimensional results of drop deformation in Stokes flow regime agreed with theoretical solutions and previous numerical results. The critical Reynolds and capillary numbers for breakup of drops were also reasonable, compared with the previous predictions. In the simulations of 3D two-drop interaction, it was shown that the breakup motion depends on not only number density of drops but also the initial positioning of their volumetric center away from a halfway cross section between the plates.

REFERENCES

[1] McNamara,G., Zanetti,G., 1988, "Use of the Boltzmann equation to simulate lattice-gas automata," Phy.Rev.Lett., 61, pp.2332-2335.

[2] Chen, S., Doolen,G.D.,1998,"Lattice Boltzmann method for fluid flows," Annu.Rev.Fluid Mech., 30, pp.329-364.

[3] Frisch, U., Hasslacher, B., Pomeau, Y., 1986, "Lattice-gas automata for the Navier-Stokes equation," Phys.Rev. Lett., 56, pp.1505-1508.

[4] Swift, M. R. ,Osborn, W.R., Yeomans, J.M., 1995, "Lattice Boltzmann simulation of nonideal fluids," Phys.Rev.Lett., 75, pp.830-833.

[5] Swift, M.R., Orlandini,E. Osborn,W.R., Yeomans, J.M., 1996, "Lattice Bolztammn simulations of liquid-gas and binary fluid systems," Phys.Rev., E 54, pp.5041-5052.

[6] Gonnella, G., Orlandini, E., Yeomans, J.M., 1997, "Lattice-Boltzmann simulations of complex fluids," Int. Modern Phys. C, 8, pp.783-792.

[7] Inamuro, T., Konishi, N., Ogino, F., 2000, "A Galilean invariant model of the lattice Boltzmann method," Comp.Phys.Communications, 129, pp.32-45.

[8] Seta, T., Takahashi, R., Takegoshi, E., Okui,K., 2002, "Thermal lattice Boltzmann simulation of bubbles rising in liquids," Proc.5th JSME-KSME Fluids Engineering Conference, No.02-57.

[9] Seta, T., Kono, K., Chen S., "Lattice Boltzmann method for two-phase flows," Int. J. Modern Phys. B, as Proc. 11th Int. Conf. on Discrete Simulation of Fluid Dynamics and Soft Condensed Matter, 2002, in press.

[10] Jamet, D., Lebaique, O., Coutris, N., Delhaye, J.M., 2001, "The second gradient method for the direct numerical simulation of liquid-vapor flows with phase change," J.Comp.Phys., 169, 624-651.

[11] Takada, N., Misawa, M., Tomiyama, A., Fujiwara, S., 2000, "Numerical simulation of two- and three-dimensional two-phase fluid motion by lattice Boltzmann method," Comp. Phys. Communications, 129, pp.233-246.

[12] Takada, N., Misawa, M., Tomiyama, A., Hosokawa, S., 2001, "Simulation of bubble motion under gravity by lattice Boltzmann method," J.Nucl.Sci.Tech.,38, pp.330-341.

[13] Hirt, C.W., Nichols, B.D., 1981, "Volume of fluid (VOF) method for the dynamics of free boundaries," J.Comp.Phys., 39, 201-225.

[14] Takada, N., Tomiyama, A., Hosokawa, S., 2001, "Three-dimensional simulation of bubble motion by lattice Boltzmann method," Proc. ASME Fluid Eng. Div. Summer Meeting, FED-Vol.254, FEDSM2001-18179.

[15] Takada, N., Tomiyama, A., Hosokawa, S., 2002, "Lattice Boltzmann simulation of interfacial deformation," Int. J. Modern Phys. B, as Proc. 11th Int. Conf. on Discrete Simulation of Fluid Dynamics and Soft Condensed Matter, 2002, in press.

[16] Li, J., Renardy, Y.Y., Renardy, M., 2000, "Numerical simulation of breakup of a viscous drop in simple shear flow through a volume-of-fluid method," Phys.Fluids, 12, pp.269-282.

[17] Cox, R.G., 1969, "The deformation of a drop in a general time-dependent fluid flow," J.Fluid Mech., 37, pp.601-623.

[18] Cao,N., Chen,S., Jin,S., Martinez,D., 1997, "Physical symmetry and lattice symmetry in lattice Boltzmann method," Phys.Rev. E, 55, pp.21-24.

[19] Chen, S., Martinez, D., 1996, "On boundary conditions in lattice Boltzmann methods," Phys.Fluids, 8, pp.2527-2536.